Direct Radiative Effect of Dust in China on Precipitation in the UCLA AGCM

Yu Gu and K. N. Liou

Department of Atmospheric and Oceanic Sciences
and Joint Institute for Regional Earth System Science and Engineering
University of California, Los Angeles, Los Angeles, California

Model Description

UCLA AGCM

- **Physical Parameterizations**
  Planetary boundary layer processes: Suarez et al. (1983), Li et al. (1999, 2001)
  Cumulus Convection: Prognostic Arakawa-Schubert (Pan and Randall 1998), with downdrafts (Cheng and Arakawa 1997)
  Radiation: Harshvardhan et al. (1987) (Control run) → Fu and Liou (1992, 1993), Gu et al. (2003)
  Prognostic Cloud Water/Ice: Kohler (1999) + Fractional clouds/Cloud overlap (Gu et al. 2003)
  Gravity Water Drag: Kim and Arakawa (1995)
- **Dynamics**
  Horizontal Finite Difference Scheme: Arakawa and Lamb (1981)
  Resolution: 5° longitude x 4° latitude
  Vertical Finite Difference Scheme: Suarez and Arakawa (1983)
  Resolution (top at 1 hPa): 15 layers
  Time integration: Leapfrog, Matsuno
- **Surface Conditions**
  Prescribed sea surface temperatures (Rayner et al. 1995), albedo, ground wetness, and surface roughness (Dorman and Sellars 1989)

Parameterization of Aerosol Effect

➢18 aerosol types: maritime, continental, urban, five different sizes of mineral dust, insoluble, water soluble, soot (black carbon), sea salt in two modes (accumulation mode and coarse mode), mineral dust in four different modes (nucleation mode, accumulation mode, coarse mode, and transported mode), and sulfate droplets.

➢Parameterized by using the recent addition of the Optical Properties of Aerosols and Clouds (OPAC) database (d'Almeida et al. 1991; Tegen and Lacis 1996; Hess et al. 1998), which provides the single-scattering properties for spherical aerosols computed from the Lorenz-Mie theory in which humidity effects are accounted for.

➢The single-scattering properties of 18 aerosol types for 60 wavelengths in the spectral region between 0.3 μm and 40 μm were interpolated into the Fu-Liou spectral bands. These properties are vertically distributed and dependent on the aerosol type and relative humidity.

Design of Experiment

Experiment	Aerosol Optical Depth	Aerosol Composition
CTRL	0.0 (Aerosol direct radiative effect not included)	None
DUST	Observed aerosol optical depths at the wavelength of 0.75 μm over China; background aerosol optical depth of 0.2 for areas other than China	100% Dust (8 μm)

Black carbon contributed about 11% to the visible optical depth of the Indo-Asian aerosols with a single-scattering albedo of ~ 0.9 both inland and over open ocean (Ramanathan et al. 2001).

Aerosol Observations in China

➢**Mineral dust** aerosols, an amount up to 30 to 50% originated from anthropogenic activities (Tegen and Fung 1995).

➢Yearly and monthly mean aerosol optical depths at the wavelength of 0.75 μm over China have been determined from the data involving the daily direct solar radiation, sunshine duration, surface pressure, and vapor pressure from 1961 to 1990 (Luo et al. 2001). Larger aerosol optical depths are found in southern China.

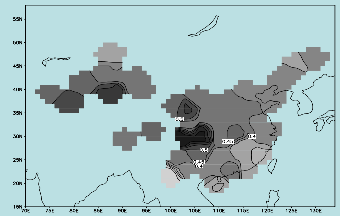

Fig. 1 Observed annual mean aerosol optical depth in China.

Summary

Dust particles absorb substantial solar radiation and have a positive solar forcing at the top of the atmosphere, but a negative solar forcing at the surface.

Increasing dust in China would produce additional heating in the air column of mid- to high latitudes and tend to move the simulated precipitation inland, i.e., toward the Himalayas.

Incorporating a large loading of dust particles in China increases simulated precipitation in northwestern China where it is normally dry, and hence tends to reduce the occurrence of dust storms. The total number of dust storm occurrence days observed between 1961 to 2003 in China has been decreasing since 1975 (Zeng et al. 2006). The present simulation results for precipitation and its impact on dust storm occurrence match the observed patterns in northwestern China.

Simulation Results

Global Mean Differences

		DUST - CTRL
Precipitation (mm day^{-1})	January	-0.84
	July	-0.59
Cloud Cover (%)	January	-6.86
	July	-7.30
Surface Air Temperature (K)	January	3.03
	July	2.13
Planetary Albedo (%)	January	-8.21
	July	-7.13

Positive solar radiative forcing is found at TOA due to the absorption of solar radiation by dust aerosols, leading to a significant decrease in planetary albedo, and increase in global surface air temperature, revealing that dust has a significant warming effect.

Observations have shown that precipitation and surface air temperature have been continuously increased in northwestern China since 1970s. Our GCM simulation results with the inclusion of dust radiative effect are in agreement with changes in the observed precipitation and temperature patterns.

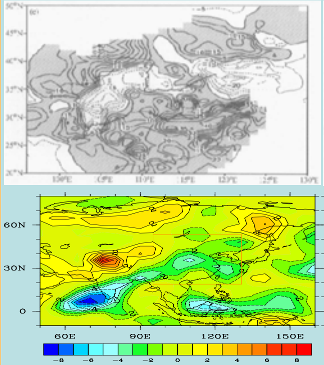

Fig. 2 Observed anomalies in precipitation (JJA) in China and the simulated July mean difference in precipitation (DUST – CTRL).

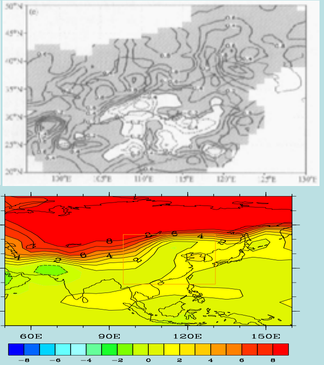

Fig. 3 Observed anomalies in surface air temperature (JJA) in China and the simulated July mean difference in surface air temperature (DUST – CTRL).

Cloud cover increases over northwestern China where precipitation is enhanced, while the corresponding solar radiation reaching the surface is reduced due to increased cloud cover.

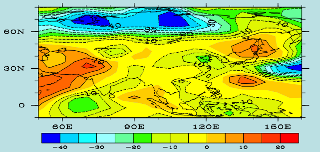

Fig. 4 July mean differences in cloud cover (DUST – CTRL).

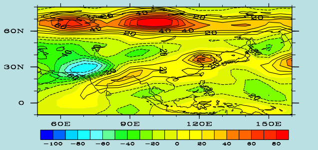

Fig. 5 July mean differences in net surface solar radiation (DUST – CTRL).